

RME8E21

L. King
COPY NO. 148
RM No. E8E21

~~CONFIDENTIAL~~

AIRESEARCH MANUFACTURING CO.

9851-9951 SEPULVEDA BLVD.

INGLEWOOD,
CALIFORNIA



[Handwritten signature]

E8E21

RESEARCH MEMORANDUM

INVESTIGATION OF PERFORMANCE OF BUMBLEBEE 18-INCH RAM JET

WITH A CAN-TYPE FLAME HOLDER

By W. H. Sterbentz and T. J. Nussdorfer

Flight Propulsion Research Laboratory
Cleveland, Ohio

INGLEWOOD,
CALIFORNIA
9851-9951 SEPULVEDA BLVD.
AIRESEARCH MANUFACTURING CO.

TECHNICAL LIBRARY

CLASSIFIED DOCUMENT

This document contains classified information affecting the National Defense of the United States within the meaning of the Espionage Act, USC 50:31 and 32. Its transmission or the revelation of its contents in any manner to an unauthorized person is prohibited by law. Information so classified may be imparted only to persons in the military and naval services of the United States, appropriate civilian officers and employees of the Federal Government who have a legitimate interest therein, and to United States citizens of known loyalty and discretion who of necessity must be informed thereof.



Classification
CHANGED TO *Unclassified*
By authority of *Spec. Rep. AL #10195-25-52*
Changed by *Spec* Date *6-5-52*
CANCELLED

NATIONAL ADVISORY COMMITTEE FOR AERONAUTICS

WASHINGTON
August 24, 1948

~~CONFIDENTIAL~~

NATIONAL ADVISORY COMMITTEE FOR AERONAUTICS

RESEARCH MEMORANDUMINVESTIGATION OF PERFORMANCE OF BUMBLEBEE 18-INCH RAM JET
WITH A CAN-TYPE FLAME HOLDER

By W. H. Sterbentz and T. J. Nussdorfer

SUMMARY

The results of an investigation conducted in the Cleveland altitude wind tunnel to determine the performance of a Bumblebee 18-inch ram jet equipped with a can-type flame holder are presented. Studies were made at a pressure altitude of approximately 30,000 feet and at ram-pressure ratios equivalent to supersonic flight Mach numbers.

Kerosene and a mixture of 75-percent kerosene and 25-percent propylene oxide were the two fuels used in evaluating the combustion performance of the ram jet. The use of the kerosene - propylene oxide fuel mixture in place of kerosene improved the combustion efficiency from 50 to 67 percent at a fuel-air ratio of 0.074 and from 39 to 51 percent at a fuel-air ratio of 0.090.

The higher combustion efficiencies attained with the kerosene - propylene oxide fuel mixture resulted in improved specific fuel consumption and an increase in gas total-temperature ratio, net thrust, and net-thrust coefficient. When the fuel mixture was used, a reduced specific fuel consumption of 5.0 pounds of fuel per hour per pound of net thrust was attained at an equivalent stream Mach number of 1.36 and a combustion efficiency ent.

INTRODUCTION

Sea-level studies of a can-type flame holder in a Bumblebee 18-inch ram jet indicate promising performance characteristics (reference 1). An investigation was conducted at the NACA Cleveland laboratory to determine the performance and operating characteristics of this ram jet and flame holder at a simulated altitude of approximately 30,000 feet and ram-pressure ratios equivalent to supersonic flight speeds. The performance of one of the best combinations of can-type flame holder and fuel-injection pattern studied is reported.

In order to determine the performance improvements that might be obtained by increasing the volatility of the fuel used, the investigation was conducted with two fuels, kerosene and a mixture of kerosene and propylene oxide. The addition of propylene oxide, a fuel of high volatility, to the kerosene was expected to improve the mixing of air and fuel and increase the rate of chemical reaction thereby improving the performance of the combustion chamber.

The combustion-chamber performance results of this investigation are presented in terms of combustion efficiency and gas total-temperature ratio across the engine as a function of the combustion-chamber-inlet variables of fuel-air ratio, velocity, and pressure. Results obtained of the over-all ram-jet performance reduced to standard atmospheric conditions at sea level are presented in terms of parameters that generalize the performance of the ram jet to any desired operating condition. (See references 2 and 3.)

APPARATUS AND PROCEDURE

The Bumblebee ram jet was installed in the Cleveland altitude wind tunnel above a 15-foot chord wing, which was fastened to the wind-tunnel balance system (fig. 1). Dry air was supplied to the engine through an air duct. Air entered the duct at approximately atmospheric pressure and could be throttled to the desired ram-jet diffuser-inlet pressure. The ram jet exhausted directly into the wind tunnel and by varying the pressure altitude, various ram-pressure ratios across the engine could be obtained. A sealed slip joint between the air duct and the ram-jet diffuser permitted free movement of the model. The tunnel balance system could therefore be used to measure thrust.

The ram jet consists of a burner, a water-cooled combustion chamber, and a subsonic diffuser in which a center body is mounted (fig. 2). The diffuser has an 11.5-inch-diameter inlet, a diffuser ratio of 1.64, and an over-all length of 9.54 feet. Attached to this diffuser was a constant-area combustion chamber 18 inches in diameter and 7.12 feet long, having an outlet diameter of 17.5 inches.

A low-pressure multiple-orifice, variable-area fuel-distributor system, which is described in reference 4, was housed in the diffuser center body (figs. 2 and 3). This system was designed to distribute the fuel evenly to a number of fuel-injection tubes over a wide range of fuel flows with small changes in fuel-injection pressure. The fuel-injection pattern used in this investigation

979

consists of two basic patterns, designated 3P and 4, by the Applied Physics Laboratory of John Hopkins University, which are alternately spaced around the center body (fig. 3). The basic patterns are shown in figure 4. The fuel-injector tubes had orifice diameters of approximately 0.188 inch and the ends of the tubes were flared to prevent fuel from dribbling along the tubes as it left the injector orifices. Fuel was injected in an upstream direction 1.42 feet from the combustion-chamber inlet to permit premixing of the fuel with the air. The air scoops shown in figure 3 were not used in this investigation.

Mounted on the end of the diffuser center body at the combustion-chamber inlet was the can-type flame holder (fig. 5). The flame holder, which was developed by the Consolidated Vultee Aircraft Corporation, was based on existing knowledge and experience in the field of turbojet combustor design. This flame holder consists of a fuel-fed pilot stage at the vertex of a perforated, segmented, conical can and was attached at its base to the walls of the combustion chamber. A two-pitch alignment of the perforations was used. The pitch of the perforations is defined as the number of spirals of perforations along the axis of the flame holder. Annular slots between the segments of the flame holder admitted cooling air. The total open area of the perforations and the annular slots was 130 percent of the combustion-chamber cross-sectional area. Stainless steel 0.042 inch thick was used to fabricate the flame holder. The over-all length of the flame holder was 48.6 inches.

Ignition of the burner was provided by the fuel-fed pilot in the vertex of the flame holder. Hydrogen was injected into the pilot burner to aid in starting. The pilot was ignited by means of a spark plug.

The two fuels used in the investigation were AN-F-32, hereinafter called kerosene, and a mixture of 75-percent AN-F-32 with 25-percent propylene oxide. The lower heating value of the kerosene was 18,500 Btu per pound and 17,150 Btu per pound for the kerosene - propylene oxide mixture.

The mass air flow through the engine was computed from total pressures, static pressures, and indicated temperatures measured with a survey rake mounted downstream of the air-duct slip joint (fig. 2). Combustion-chamber-inlet velocities were computed from wall static pressures measured at the combustion-chamber inlet and from the air flow. As a check on the wind-tunnel balance system, a water-cooled combustion-chamber-outlet rake of total- and static-pressure tubes was used to obtain the jet thrust for some readings. No tunnel-balance data are presented for these readings because they

include the drag of the combustion-chamber-outlet rake. Total-pressure losses across the diffuser were obtained from two total-pressure survey rakes, one upstream and the other downstream of the fuel injectors, as shown in figure 2. The ram-jet fuel flow was measured with a rotameter.

Measured values of jet thrust and gas flow were used to compute the combustion efficiency and the gas total-temperature rise in accordance with the methods presented in references 2 and 3. The heat lost to the combustion-chamber cooling water was accounted for in the calculation of combustion efficiency. This heat loss was computed from cooling-water-flow and temperature-rise measurements.

Engine performance parameters were computed by the methods discussed in references 2 and 3. In computing equivalent free-stream Mach numbers, the losses across a normal shock at the throat of an assumed convergent-divergent supersonic diffuser of optimum contraction ratio were added to the measured diffuser-inlet total pressure to obtain the equivalent free-stream total pressure.

Data were obtained at pressure altitudes from 25,400 to 30,200 feet. Readings were taken over a range of combustion-chamber-inlet static pressures from 1871 to 1488 pounds per square foot absolute and fuel-air ratios from 0.074 to 0.092. The inlet-air total temperature was maintained at $140^{\circ} \pm 10^{\circ}$ F.

SYMBOLS

The following symbols are used in this report:

A	cross-sectional area, square feet
C_F	net-thrust coefficient, $\frac{F_n}{\frac{1}{2}\rho_0 V_0^2 A_3}$
F_j	jet thrust, pounds
F_n	net thrust, pounds

f/a	fuel-air ratio
M	Mach number
P	total pressure, pounds per square foot absolute
ΔP	total-pressure drop, pounds per square foot
P_j/P_0	total-pressure ratio across engine
p	static pressure, pounds per square foot absolute
q	dynamic pressure, pounds per square foot
T	total temperature, °R
V	velocity, feet per second
W_a	air flow, pounds per second
W_f	fuel flow, pounds per hour
δ	ratio of absolute tunnel ambient-air pressure to absolute static pressure at NACA standard atmospheric conditions at sea level, $p_0/2116$
η	over-all efficiency, percent
η_b	combustion efficiency, percent
θ	ratio of absolute total temperature at diffuser inlet to absolute static temperature at NACA standard atmospheric conditions at sea level, $T_1/519$
τ	ratio of absolute total temperature at combustion-chamber-outlet to absolute total temperature at diffuser inlet, T_4/T_1

Subscripts:

0	equivalent free-stream condition
1	subsonic-diffuser inlet
2	diffuser outlet and combustion-chamber inlet

- 4 combustion-chamber outlet
- j exhaust-jet conditions at ambient pressure ($p_j = p_0$)

Performance parameters:

- F_j/δ jet thrust reduced to NACA standard atmospheric conditions at sea level, pounds
- F_n/δ net thrust reduced to NACA standard atmospheric conditions at sea level, pounds
- $W_f/(F_n \sqrt{\theta})$ reduced specific fuel consumption, pounds fuel per hour per pound net thrust
- $F_n/(W_a \sqrt{\theta})$ reduced air specific impulse, pounds net thrust per pound air per second

RESULTS AND DISCUSSION

Ram-Jet Combustion Performance

The combustion efficiency η_b of the ram jet was markedly affected by the following variables: (1) fuel-air ratio f/a , (2) combustion-chamber-inlet velocity V_2 , and (3) the fuel used. The effect of changes in these variables on the combustion-chamber performance is shown in figures 6 and 7, where η_b and gas total-temperature ratio τ are presented as functions of f/a with kerosene and a mixture of 75-percent kerosene and 25-percent propylene oxide as fuels. These figures also give the values of V_2 and the range of combustion-chamber-inlet static pressure p_2 at which data were taken. These data were obtained with the ram jet operating at or near exhaust-nozzle-outlet choking conditions.

The lean f/a at which flame blow-out occurred was approximately 0.074 and was not noticeably affected by the fuel used. The rich f/a limit was not determined with either fuel, but stable combustion data were obtained to fuel-air ratios of 0.092. At a given value of V_2 , the combustion efficiency gradually decreased with increases in fuel-air ratio with either fuel. This decrease in η_b occurred because of overenrichment of the fuel-air mixture.

At a V_2 of approximately 245 feet per second with kerosene as the fuel, η_b decreased from approximately 50 percent at a fuel-air ratio of 0.075 to approximately 39 percent at a fuel-air ratio of 0.090 (fig. 6). When the mixture of kerosene and propylene oxide was used as a fuel, marked improvement of about 10 to 15 percent in combustion efficiency was noted (fig. 7). Concomitant increases in τ also reduced the average value of V_2 obtained. With the ram jet operating at a V_2 of approximately 230 feet per second, η_b varied from about 67 percent at a fuel-air ratio of 0.074 to about 51 percent at a fuel-air ratio of 0.090 (fig. 7(b)). The improvement in η_b obtained by using the fuel mixture may be partly attributed to the improved vaporization and mixing of the fuel and air resulting from the increased fuel volatility through the addition of propylene oxide to the kerosene. In an experiment reported in reference 5, increasing the volatility of gasoline by preheating produced a similar improvement in η_b .

At approximately constant values of V_2 and fuel-air ratio, variations in p_2 over the range investigated (1488 to 1871 lb/sq ft absolute) appeared to have little effect on η_b , as shown in figure 8. The same insensitivity of η_b to variations in p_2 over approximately the same range is reported in reference 6.

When the ram jet was operated with kerosene, flame blow-out occurred when p_2 was reduced below approximately 1480 pounds per square foot absolute. At this time, the ram jet was operating at a V_2 of about 278 feet per second, a fuel-air ratio of 0.090, and a tunnel static pressure p_0 of 650 pounds per square foot absolute. At these conditions, the combustion-chamber-outlet Mach number M_4 was subsonic and very close to 1.0. When the kerosene-propylene oxide mixture was used as fuel, p_2 could be reduced to approximately 1220 pounds per square foot absolute before flame blow-out. This blow-out point was observed when the ram jet was operating at a V_2 of about 220 feet per second, a fuel-air ratio of about 0.088, and a p_0 of 630 pounds per square foot absolute. For these conditions, M_4 was approximately 0.83.

Ram Jet Over-All Performance

The highest equivalent free-stream Mach number M_0 attained with this ram jet was 1.42. This maximum was not set by an operational limit of the engine but by the pumping capacity of the test apparatus. At this condition of M_0 , a jet thrust F_j of 1980 pounds was developed by the engine at a pressure altitude of

approximately 30,000 feet. This value is shown in figure 9(a), which presents the actual measured jet thrusts and the altitudes at which these data were obtained. The altitude contours are based on the reduced jet thrust curve of figure 9(b).

As discussed in reference 2, the jet thrust of a given ram jet is primarily a function of M_0 , pressure altitude, and the total-pressure ratio across the engine P_j/P_0 . A single curve is obtained if the quantity F_j/δ is plotted as a function of M_0 for a constant value of P_j/P_0 . Thus the quantity F_j/δ is equivalent to the sea-level jet thrust of the ram jet. The reduced jet-thrust data F_j/δ measured by two methods is shown in figure 9(b). This figure indicates that the data are relatively consistent. In the first method, the jet thrust of the ram jet was computed from the wind-tunnel-balance data and inlet-momentum considerations; in the second method, the jet thrust was computed from an integrated average of measured values of total and static pressures at the combustion-chamber outlet. The maximum F_j/δ developed by the engine was 6750 pounds.

The reduced net thrust F_n/δ and the net-thrust coefficient C_F increased rapidly with M_0 (fig. 10). At the highest equivalent free-stream Mach number attained (1.42) and at a τ of 5.4, the net thrust reduced to sea-level conditions was 3650 pounds. The corresponding C_F was 0.695. At a given value of M_0 , higher values of F_n/δ and C_F were obtained when the mixture of kerosene and propylene oxide was used as fuel because higher values of τ were obtained than when kerosene was used as fuel.

The reduced air specific impulse $F_n/(W_a \sqrt{\theta})$ and the reduced specific fuel consumption $W_f/(F_n \sqrt{\theta})$ are shown in figures 11 and 12, respectively, as a function of M_0 . The reduced air specific impulse of the engine increased with both M_0 and τ . The maximum $F_n/(W_a \sqrt{\theta})$ was 49.7 pounds of net thrust per pound of air per second at an M_0 of 1.42 and a τ of 5.4. Because of the higher values of τ attained when the kerosene - propylene oxide mixture was used, higher values of reduced air specific impulse were obtained.

Reduced specific fuel consumption decreased with increases in M_0 (fig. 12). No curves have been drawn through the data because $W_f/(F_n \sqrt{\theta})$ is also a function of η_b and τ and variations in these quantities caused the data to scatter. At M_0 of 1.42, τ of 5.4, and η_b of 60 percent, the reduced specific fuel consumption was 5.0 pounds of fuel per hour per pound of net thrust.

Improvement in η_b with the mixture of kerosene and propylene oxide resulted in generally lower values of $W_f/(F_n \sqrt{\theta})$ than with only kerosene. A value of 5.0 pounds of fuel per hour per pound of net thrust was attained at M_0 of 1.36, τ of 5.2, and η_b of 67 percent when the mixed fuel was used.

The improvement in reduced specific fuel consumption with an increase in M_0 and with the kerosene - propylene oxide fuel mixture in place of kerosene is shown in figure 13 in terms of over-all efficiency η . At M_0 of 1.36, τ of 5.2, and η_b of 67 percent, a maximum η of 7.0 percent was obtained with the kerosene - propylene oxide fuel mixture. As with the specific-fuel-consumption data, no curves have been drawn through the over-all efficiency data because variations in η_b and τ caused the data to scatter. A single curve of η can be obtained if η_b and τ are included in a parameter, as suggested in reference 3.

The effect of M_0 on the total-pressure recovery ratio across the engine P_j/P_0 is presented in figure 14. For the range of M_0 and τ over which the data were obtained, P_j/P_0 was essentially constant at about 0.71. No variation in P_j/P_0 with M_0 was obtained because the ram jet was operated at or near combustion-chamber-outlet choking conditions. Included in P_j/P_0 are the assumed supersonic diffuser total-pressure recoveries, which amount to 0.99 at an M_0 of 1.40. A discussion and an evaluation of the various types of pressure losses in a ram jet are given in references 3 and 7.

Measured total-pressure drop coefficients $\Delta P/q_2$ over the subsonic diffuser with the fuel injector in place and over the combustion chamber and the flame holder were obtained from drag studies without combustion. These coefficients are presented in figure 15 as a function of combustion-chamber-inlet Mach number M_2 . The subsonic-diffuser total-pressure drop coefficient increased with M_2 from about 1.35 at M_2 equal to 0.05 to about 1.85 at 0.16. Over the same range of M_2 , the total-pressure drop coefficient over the combustion chamber and the flame holder was approximately constant at about 1.5. No measurements of these pressure-drop coefficients were obtained with combustion.

The M_0 at which a choking condition at the combustion-chamber outlet was attained is illustrated in figure 16, which gives the variation of the ultimate exhaust-jet Mach number M_j with M_0 .

An M_j of 1.0 occurred at an M_0 of 1.24. Choking condition was not reached at an M_0 of 1.0 primarily because of the loss in total pressure through the engine.

SUMMARY OF RESULTS

The following results were obtained from an investigation of the performance of a Bumblebee 18-inch ram jet with a can-type flame holder, which operated at a pressure altitude of approximately 30,000 feet and at ram-pressure ratios equivalent to supersonic flight Mach numbers with both kerosene and a mixture of kerosene and propylene oxide as fuels:

1. The combustion efficiency improved when the kerosene - propylene oxide fuel mixture was substituted for kerosene as the fuel. At a fuel-air ratio of about 0.074, the combustion efficiency increased from approximately 50 to 67 percent and at a fuel-air ratio of 0.090 the combustion efficiency was increased from approximately 39 to 51 percent. Concomitant increases in the total-temperature ratio across the engine were also obtained.

2. At approximately constant values of combustion-chamber-inlet velocity and fuel-air ratio, variations in combustion-chamber-inlet pressure over the range investigated (1488 to 1871 lb/sq ft absolute) appeared to have little effect on combustion efficiency.

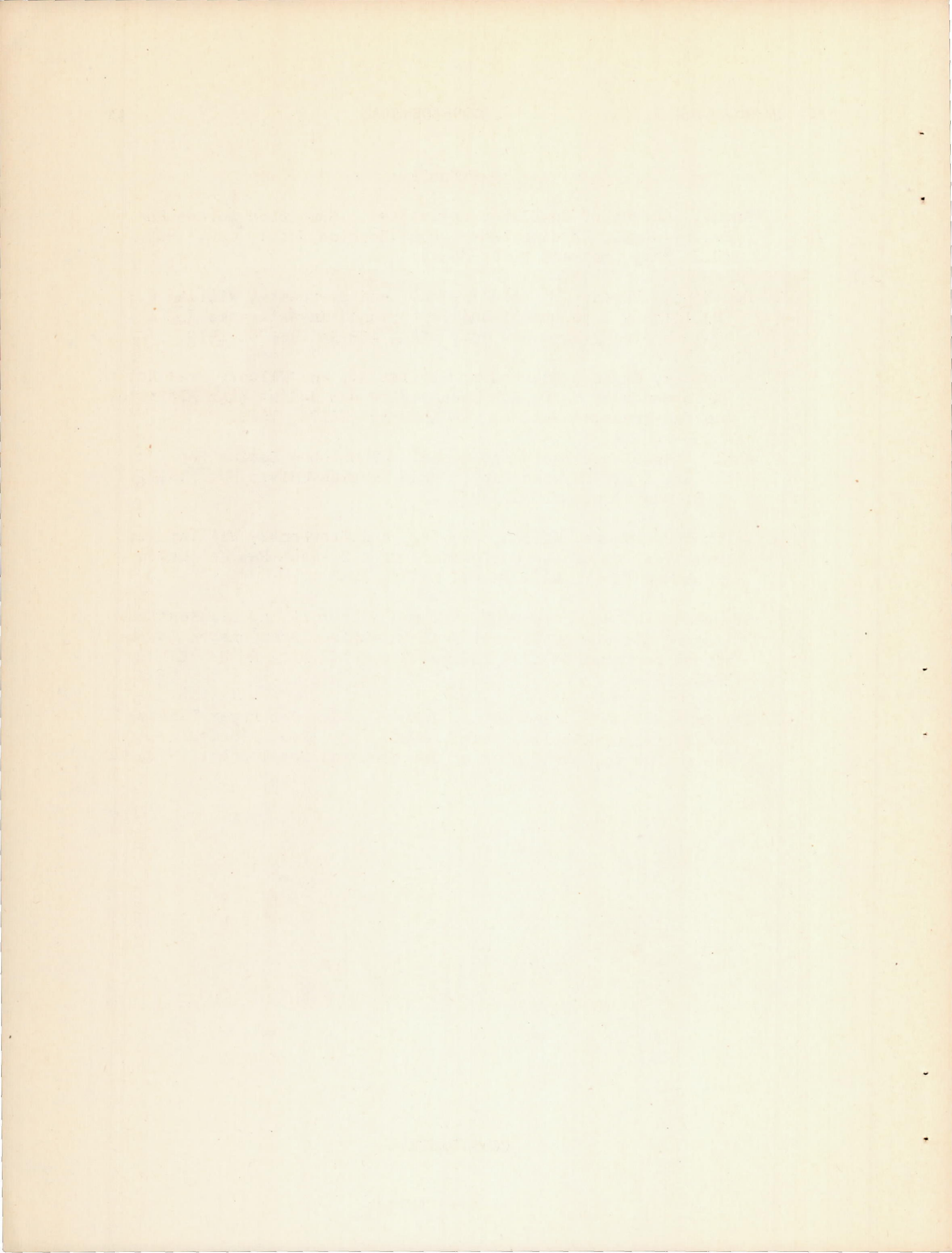
3. The lean fuel-air ratio of approximately 0.074 at which flame blow-out occurred was not noticeably affected by the fuel used. No rich fuel-air-ratio limit was determined with either fuel, but stable combustion data were obtained at fuel-air ratios of 0.092.

4. The higher combustion efficiencies attained with the kerosene - propylene oxide fuel mixture resulted in an improvement in specific fuel consumption and increases in gas total-temperature ratio, net thrust, and net-thrust coefficient as compared with those attained with kerosene. When using the fuel mixture, a reduced specific fuel consumption of 5.0 pounds of fuel per hour per pound of net thrust was attained at an equivalent free-stream Mach number of 1.36 and a combustion efficiency of 67 percent.

Flight Propulsion Research Laboratory,
National Advisory Committee for Aeronautics,
Cleveland, Ohio.

REFERENCES

1. Anon.: Survey of Bumblebee Activities. Bumblebee Series Rep. No. 69, Appl. Physics Lab., Johns Hopkins Univ., Oct. 1947. (U.S. Navy Contract NOrd 7386.)
2. Perchonok, Eugene, Wilcox, Fred A., and Sterbentz, William H.: Preliminary Development and Performance Investigation of a 20-Inch Steady-Flow Ram Jet. NACA ACR No. E6D05, 1946.
3. Perchonok, Eugene, Sterbentz, William H., and Wilcox, Fred A.: Performance of a 20-Inch Steady-Flow Ram Jet at High Altitudes and Ram-Pressure Ratios. NACA RM No. E6L06, 1947.
4. Anon.: Bumblebee Equipment Manual. Bumblebee Series Rep. No. 62, Appl. Physics Lab., Johns Hopkins Univ., Nov. 1947. (U.S. Navy Contract NOrd 7386.)
5. Perchonok, Eugene, Wilcox, Fred A., and Sterbentz, William H.: Investigation of the Performance of a 20-Inch Ram Jet Using Preheated Fuel. NACA RM No. E6I23, 1946.
6. Sterbentz, W. H., Perchonok, E., and Wilcox, F. A.: Investigation of Effects of Several Fuel-Injection Locations on Operational Performance of a 20-Inch Ram Jet. NACA RM No. E7L02, 1948.
7. Williams, Glenn C., and Quinn, John C.: Ram Jet Power Plants. Jet Propelled Missiles Panel, OSRD. May 1945. (Under Assignment to Coordinator of Research and Development, U.S. Navy.)



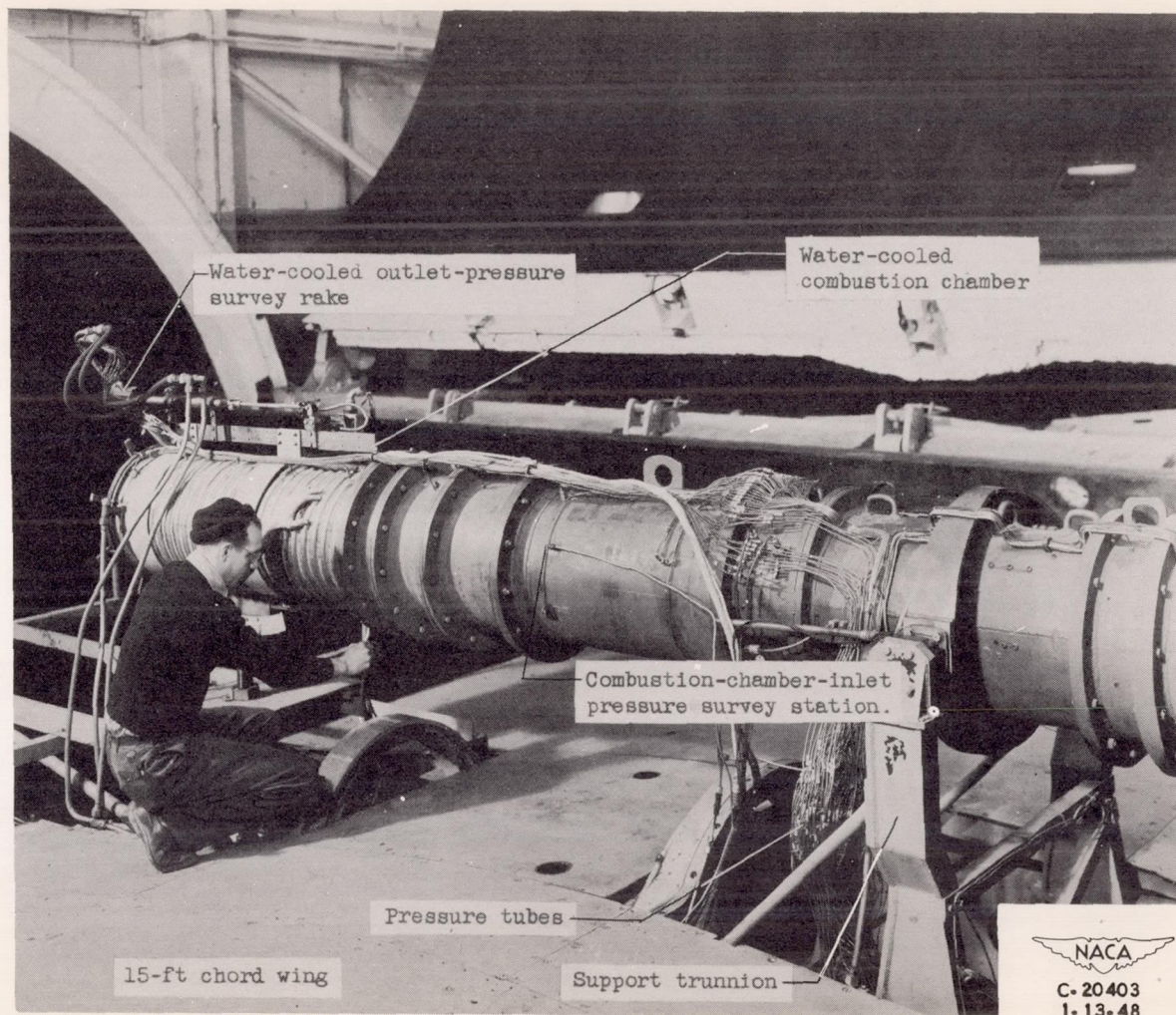
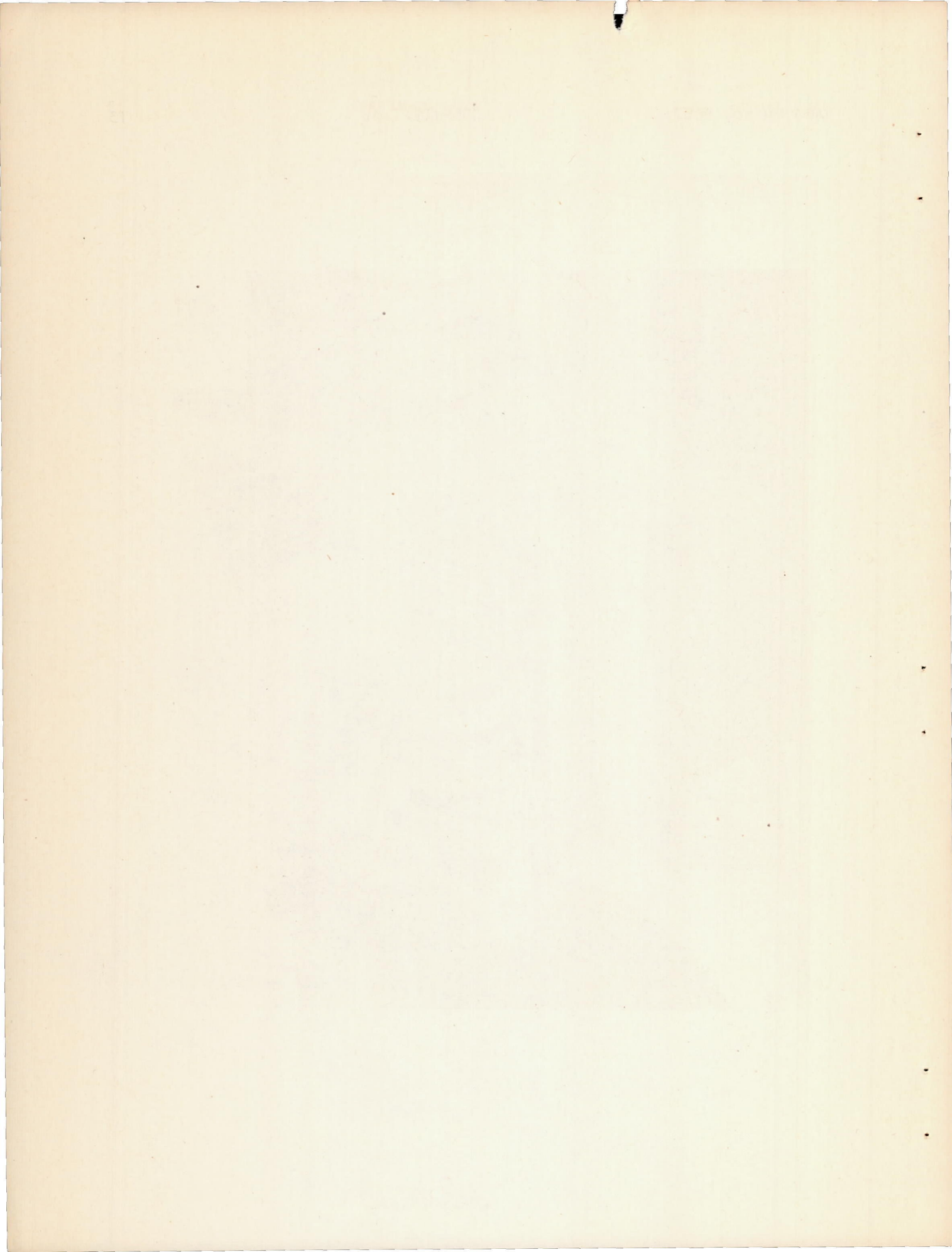
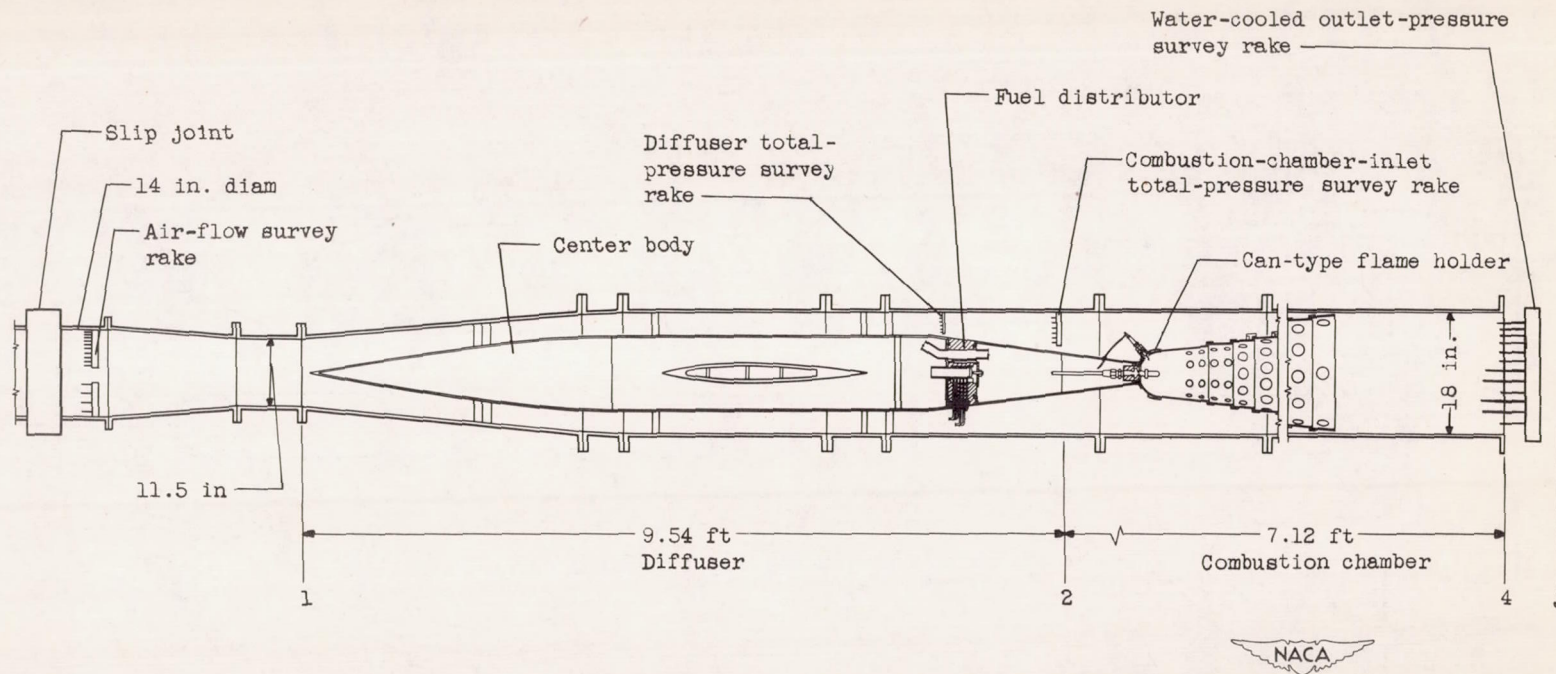


Figure 1. - Installation of Bumblebee 18-inch ram jet in altitude wind tunnel.



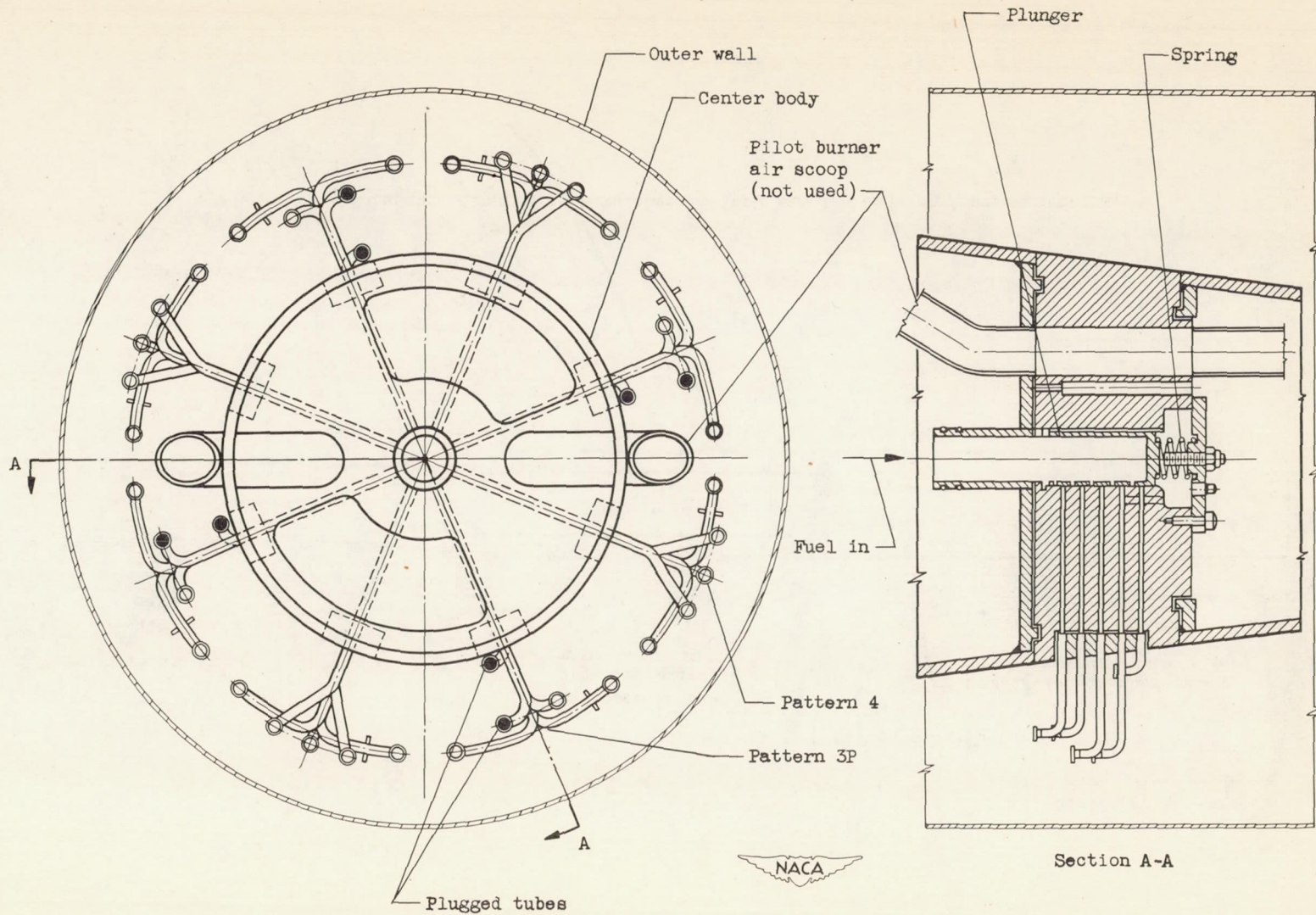
CONFIDENTIAL



CONFIDENTIAL

Figure 2. - Schematic diagram of Bumblebee 18-inch ram jet showing instrumentation.

CONFIDENTIAL

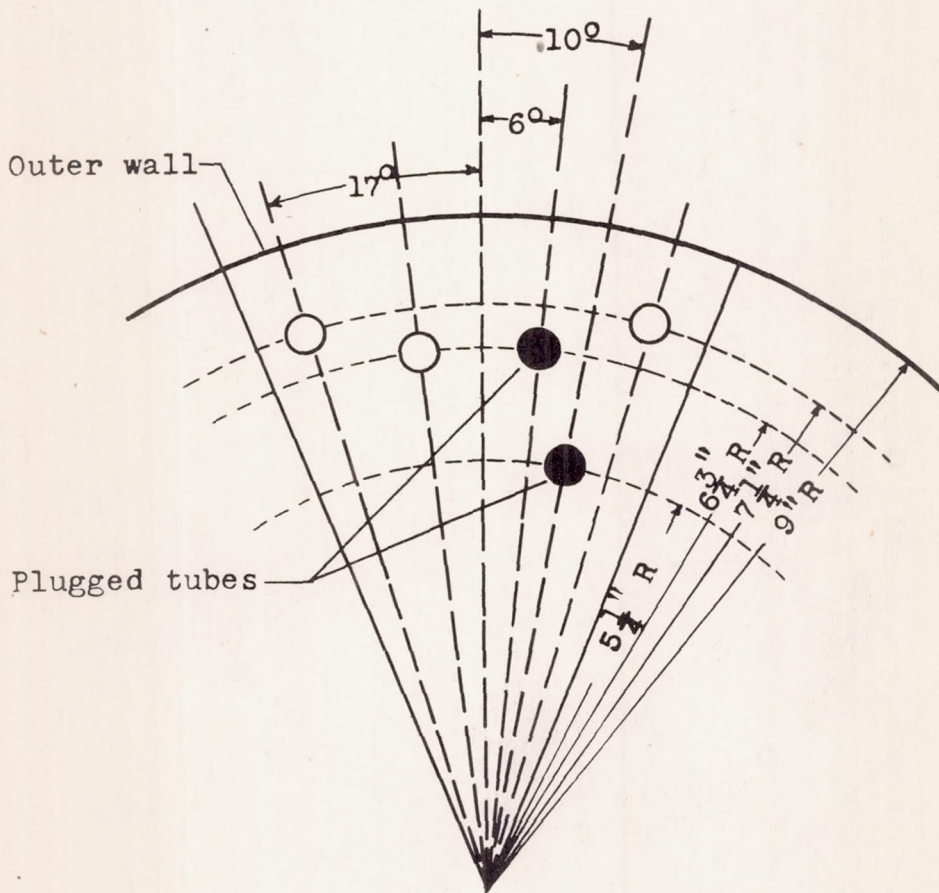


16

CONFIDENTIAL

NACA RM No. E8E21

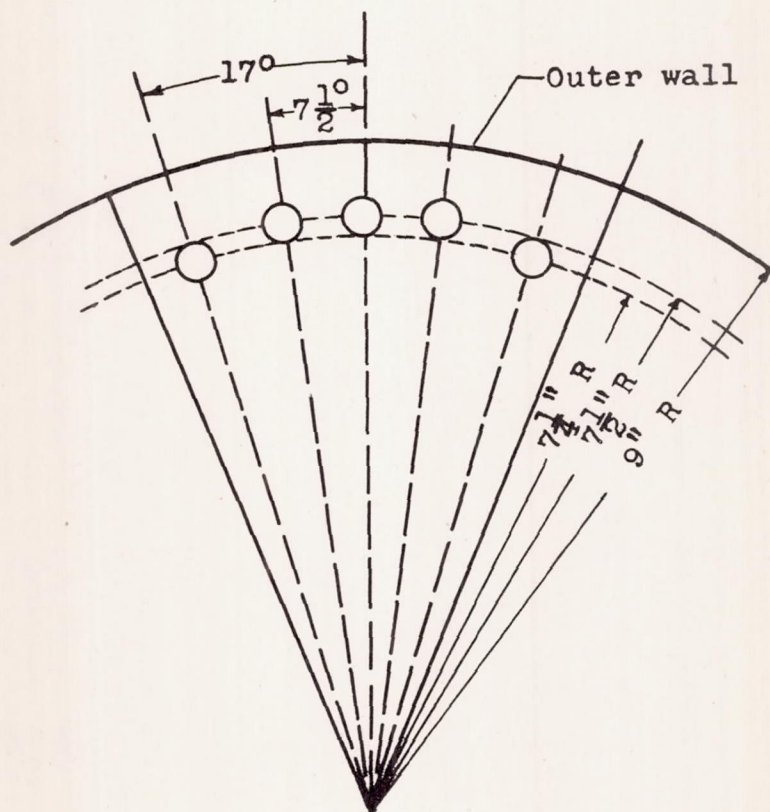
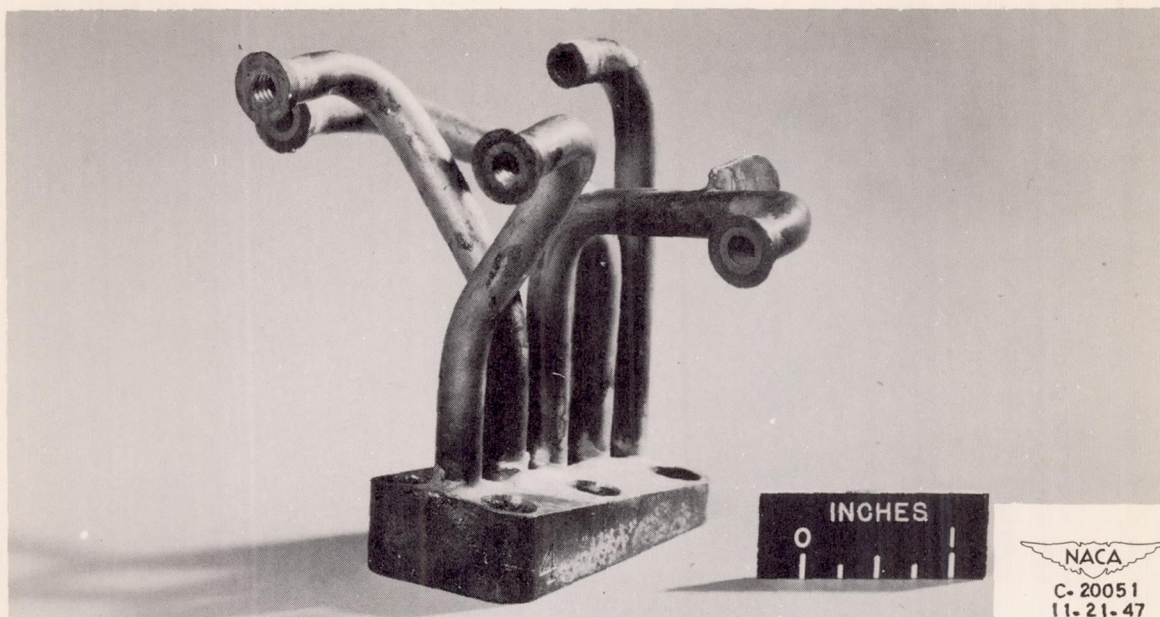
Figure 3. - Schematic diagram of multiple-orifice, variable-area fuel-distributor system and fuel-injection pattern.



(a) Fuel pattern 3P.

Figure 4. - Photograph and schematic diagram of fuel patterns.

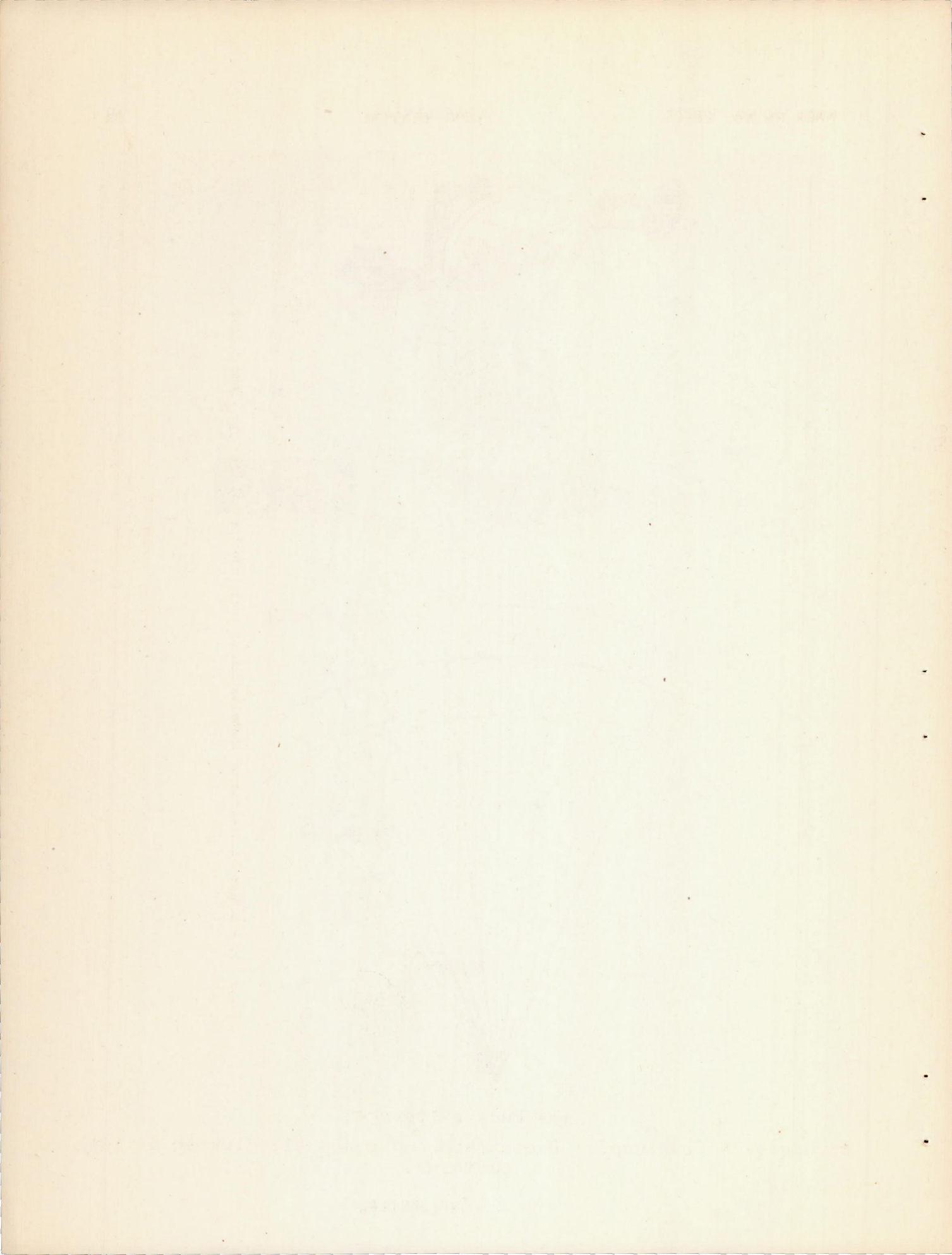
979



(b) Fuel pattern 4.

Figure 4. - Concluded. Photograph and schematic diagram of fuel patterns.

979



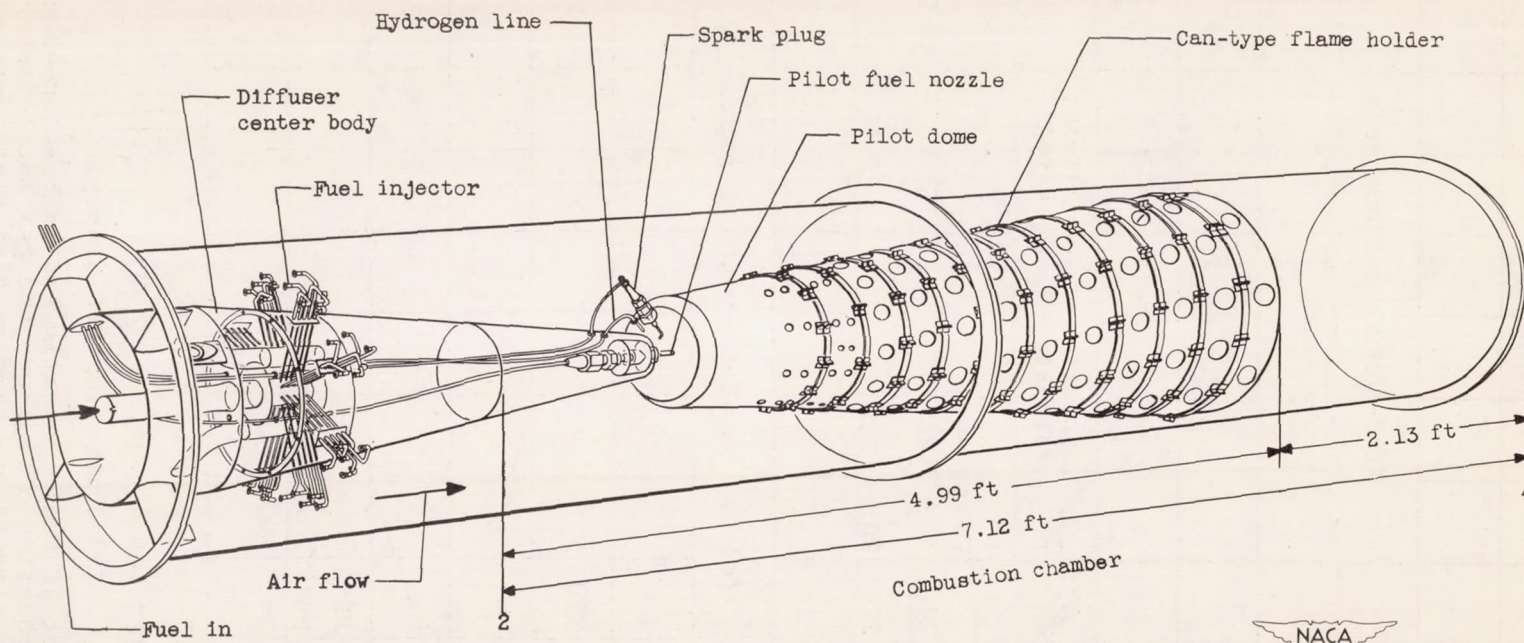
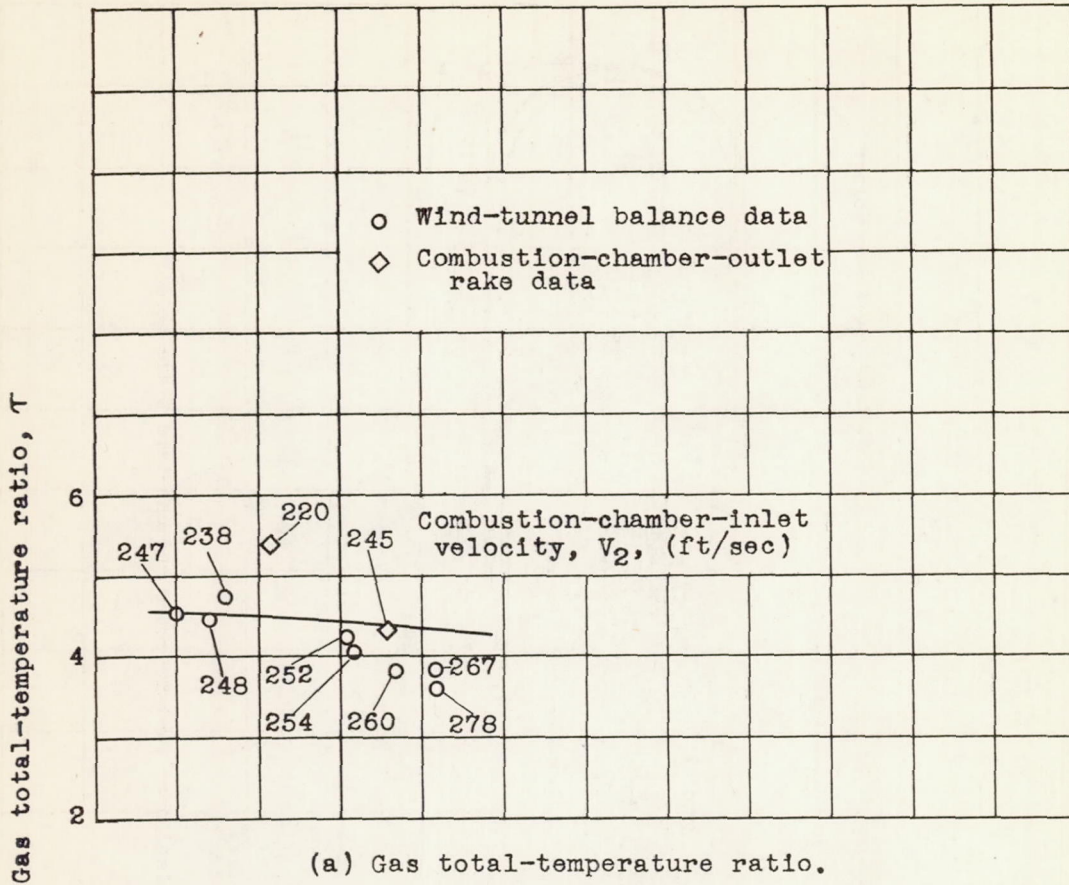
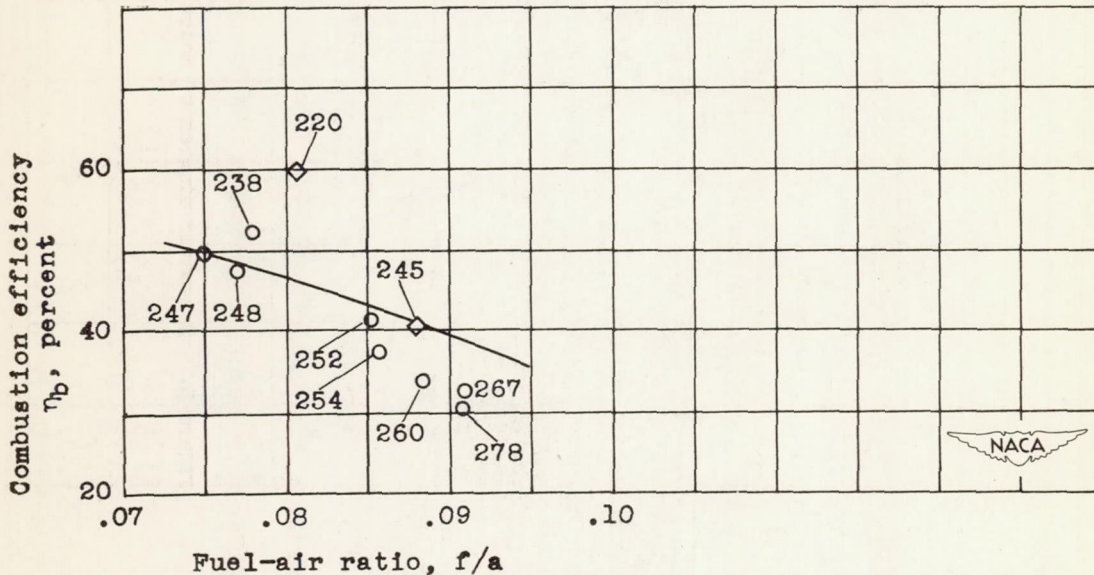


Figure 5. - Schematic diagram of installation of fuel injector and can-type flame holder.



(a) Gas total-temperature ratio.



(b) Combustion efficiency.

Figure 6. - Effect of fuel-air ratio and combustion-chamber-inlet velocity on combustion efficiency and gas total-temperature ratio. Fuel, kerosene; combustion-chamber-inlet static pressure, 1488 to 1871 pounds per square foot absolute.

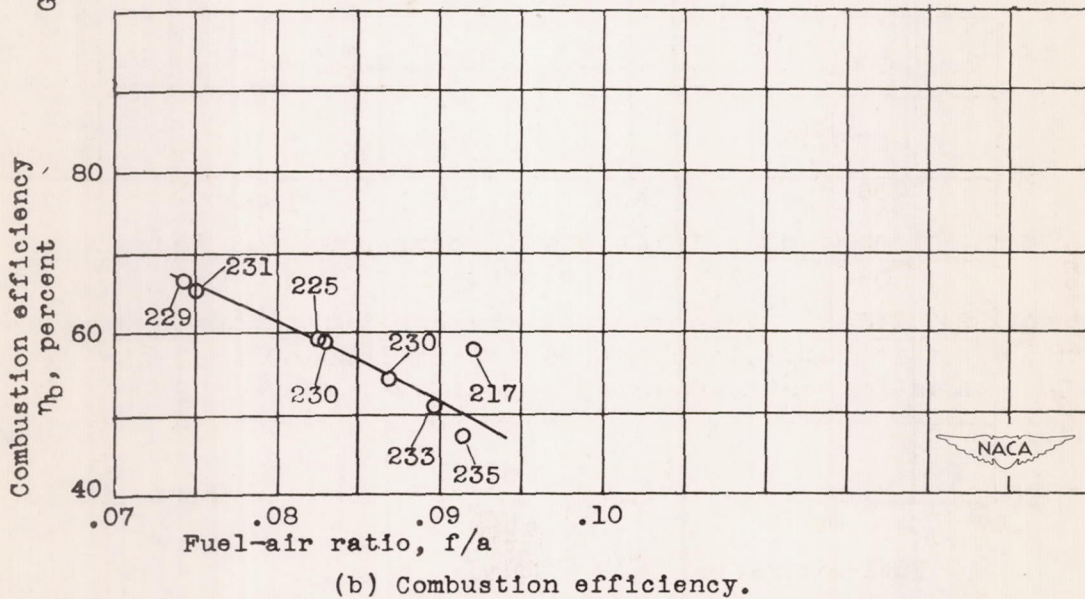
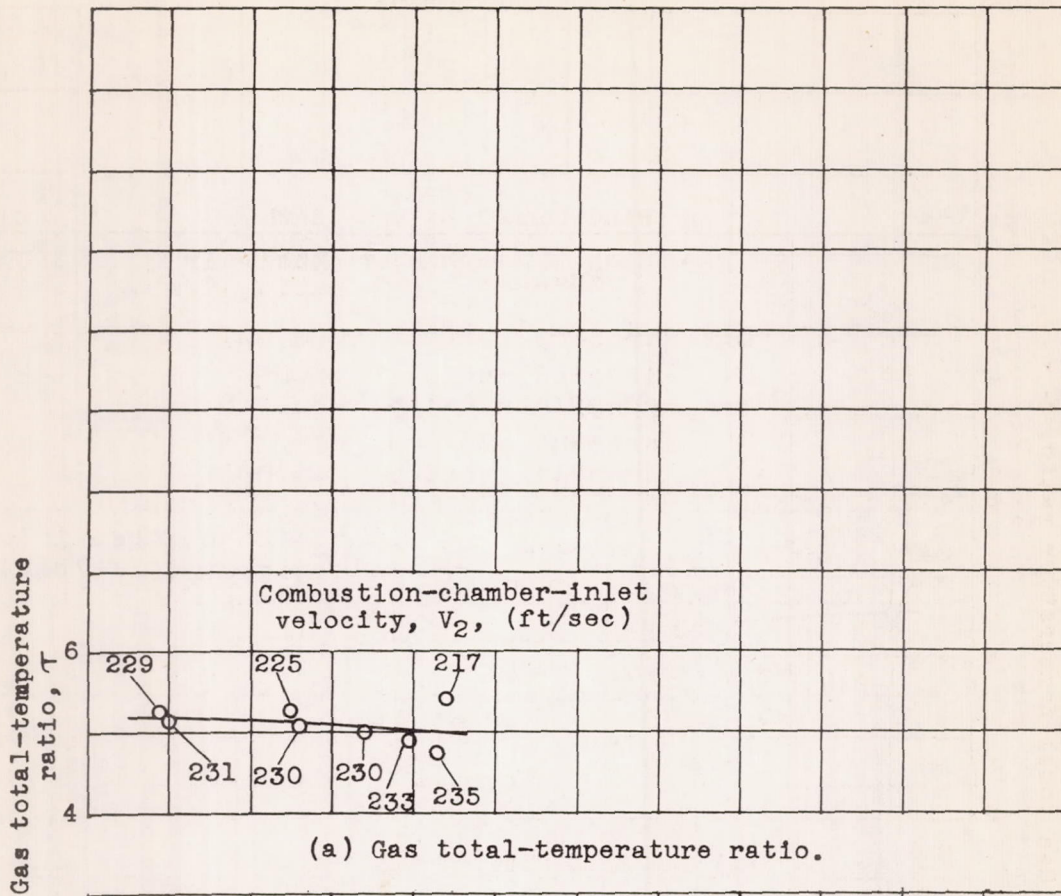


Figure 7. - Effect of fuel-air ratio and combustion-chamber-inlet velocity on combustion efficiency and gas total-temperature ratio. Fuel, 75-percent kerosene and 25-percent propylene oxide; combustion-chamber static pressure, 1561 to 1725 pounds per square foot absolute.

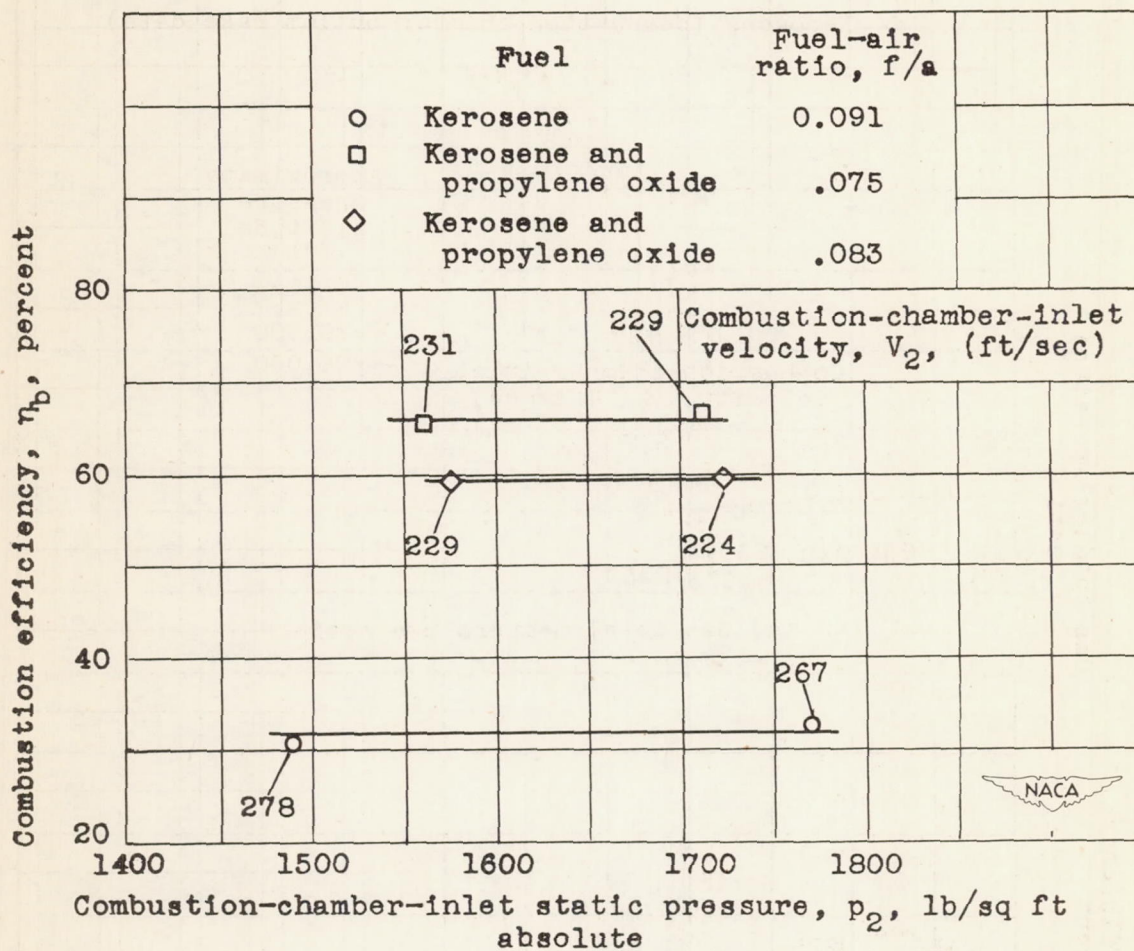
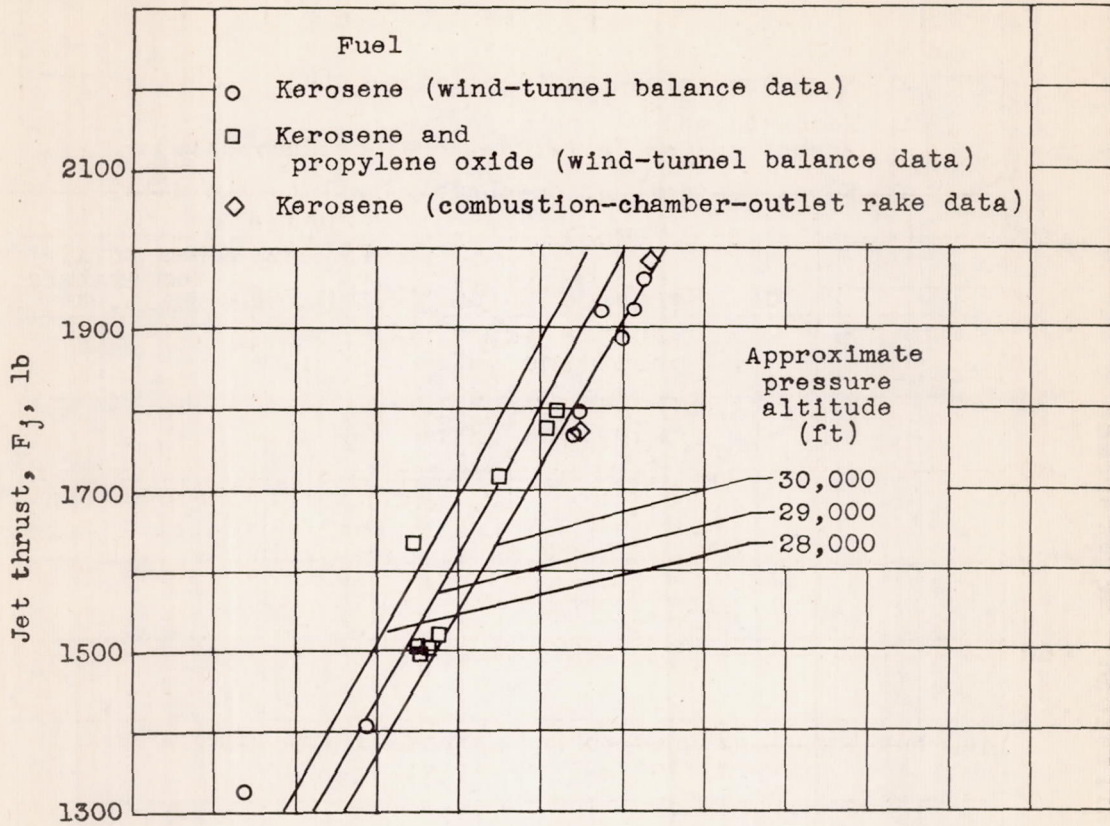
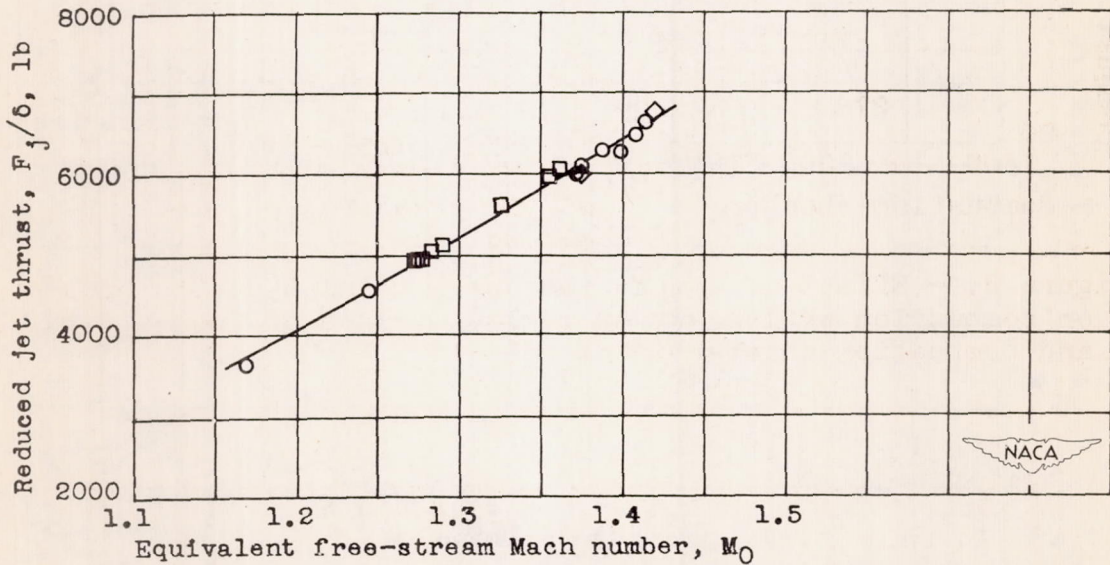


Figure 8. - Effect of combustion-chamber-inlet static pressure on combustion efficiency at various values of fuel-air ratio and combustion-chamber-inlet velocity.

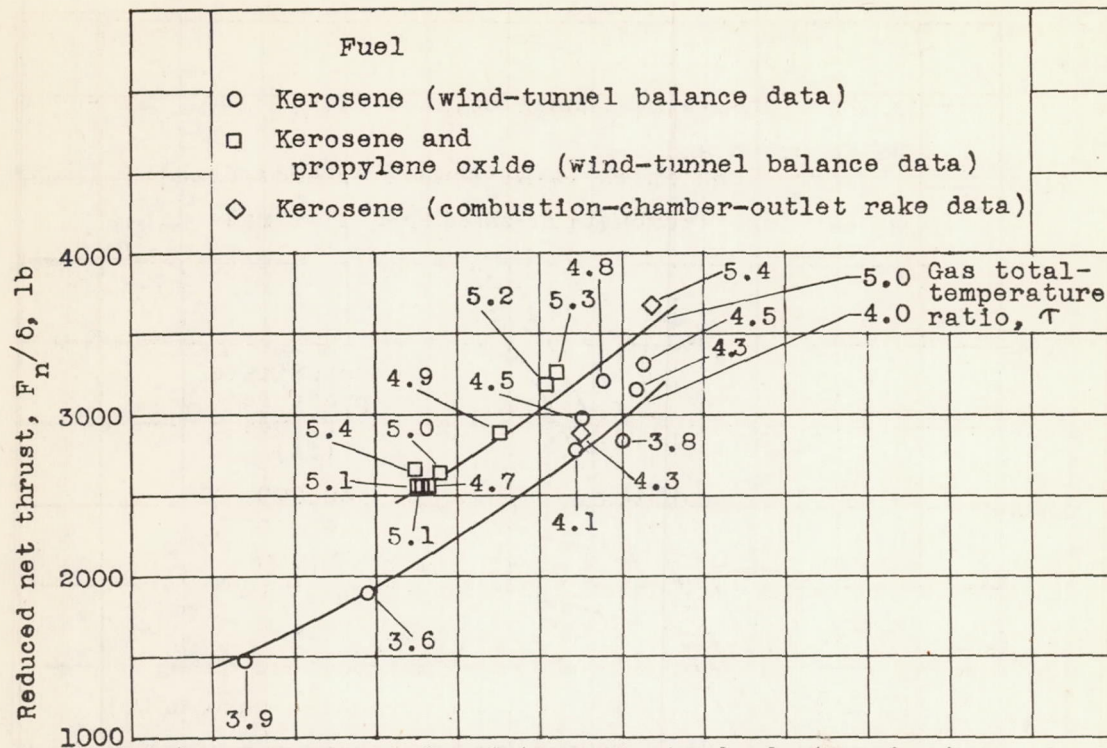


(a) Jet thrust.

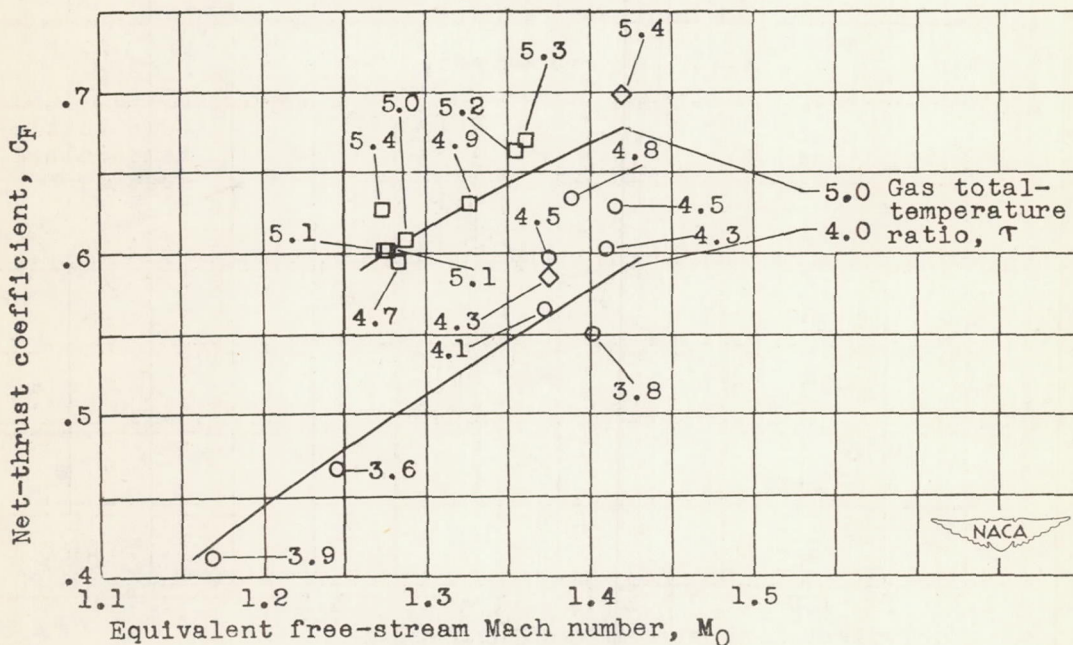


(b) Jet thrust reduced to NACA standard atmospheric conditions at sea level.

Figure 9. - Effect of equivalent free-stream Mach number and pressure altitude on jet thrust and reduced jet thrust.



(a) Net thrust reduced to NACA standard atmospheric conditions at sea level.



(b) Net thrust coefficient.

Figure 10. - Effect of equivalent free-stream Mach number, gas total-temperature ratio, and fuel on reduced net thrust and net-thrust coefficient.

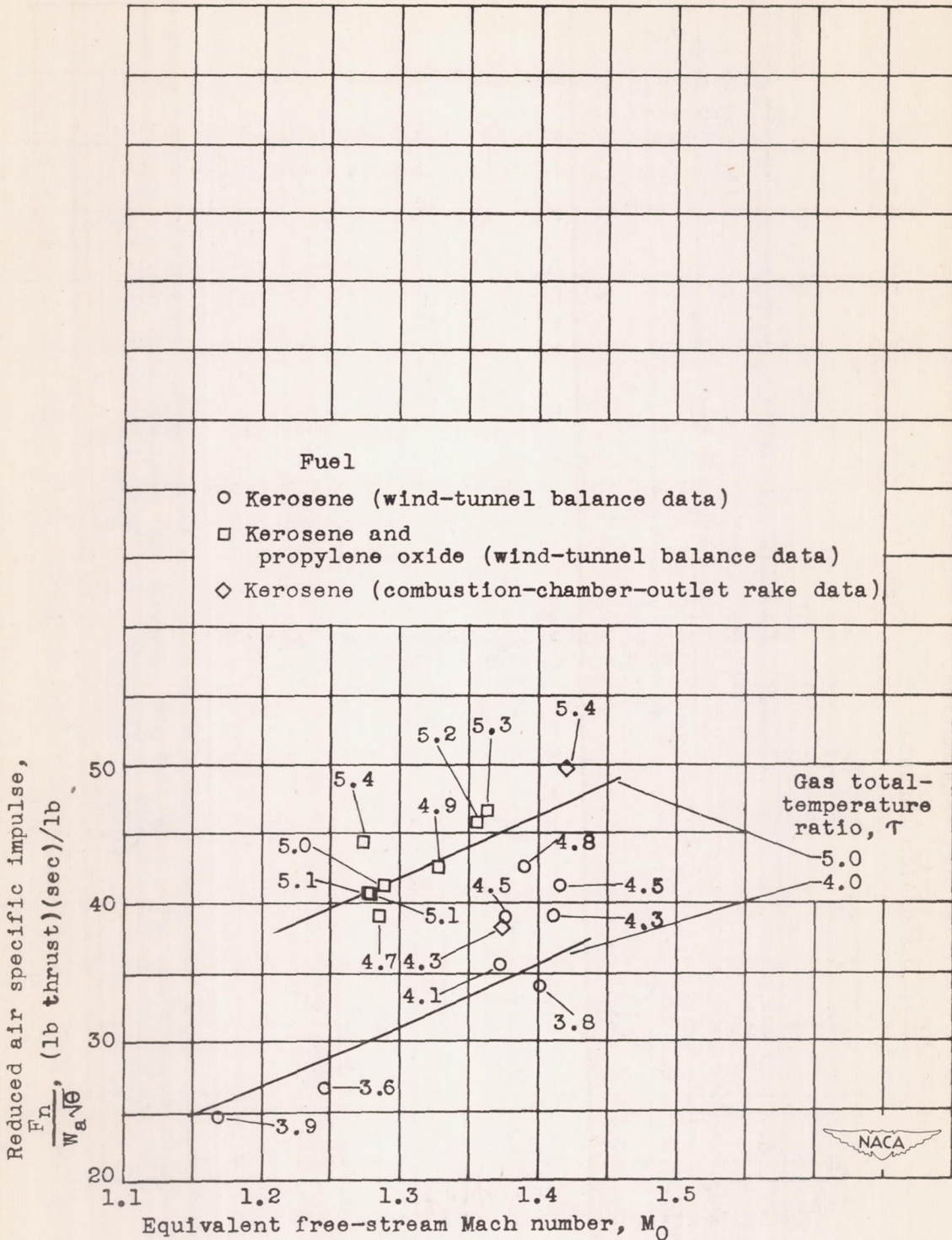


Figure 11. - Effect of equivalent free-stream Mach number, gas total-temperature ratio, and fuel on air specific impulse reduced to NACA standard atmospheric conditions at sea level.

979

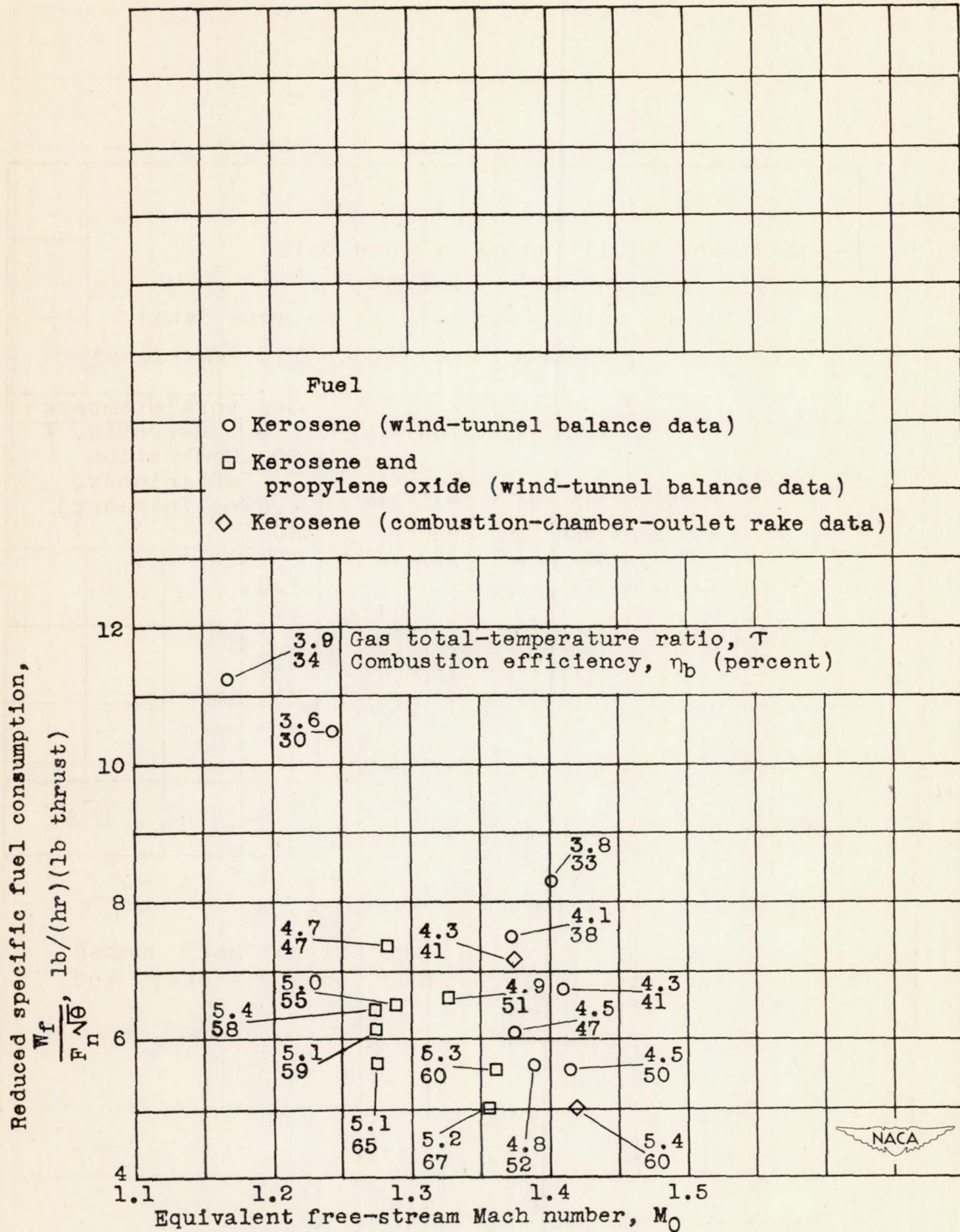


Figure 12. - Effect of equivalent free-stream Mach number, gas total-temperature ratio, combustion efficiency, and fuel on specific fuel consumption reduced to NACA standard atmospheric conditions at sea level.

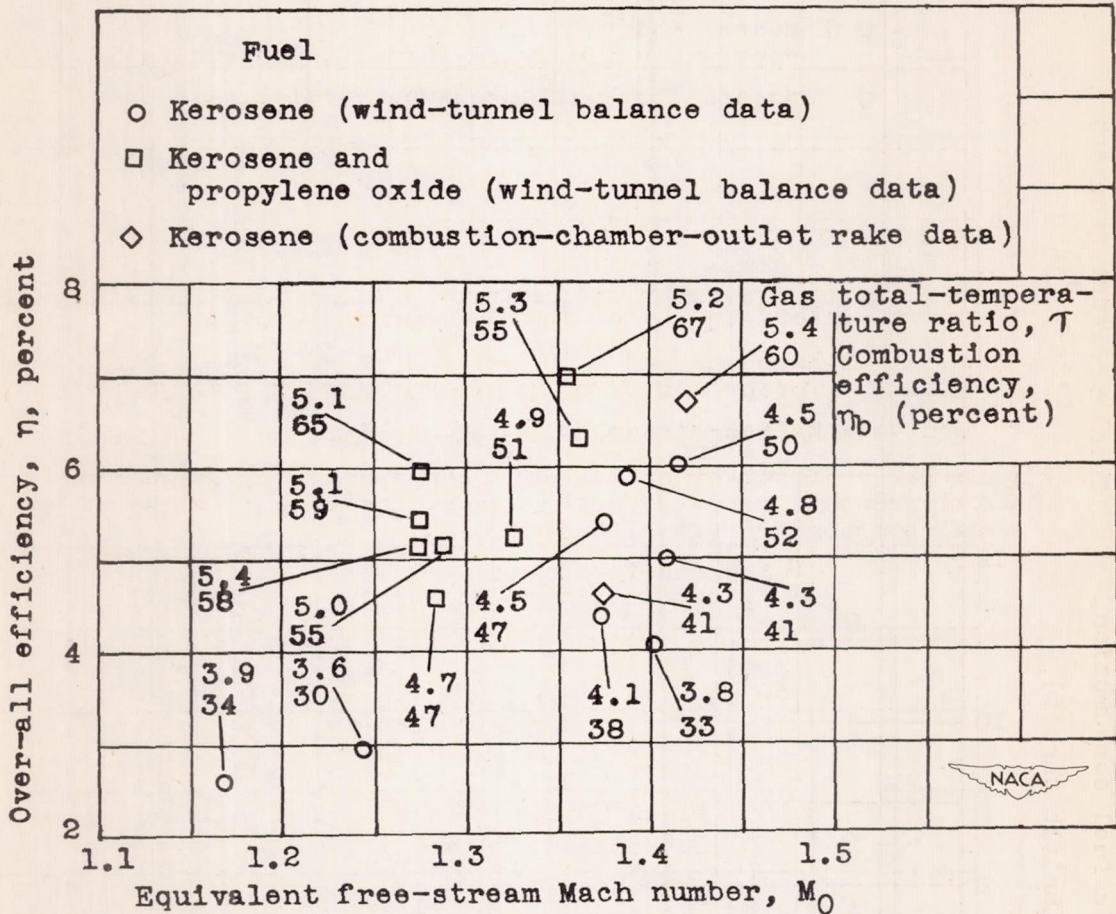


Figure 13. - Effect of equivalent free-stream Mach number, gas total-temperature ratio, combustion efficiency, and fuel on over-all efficiency.

979

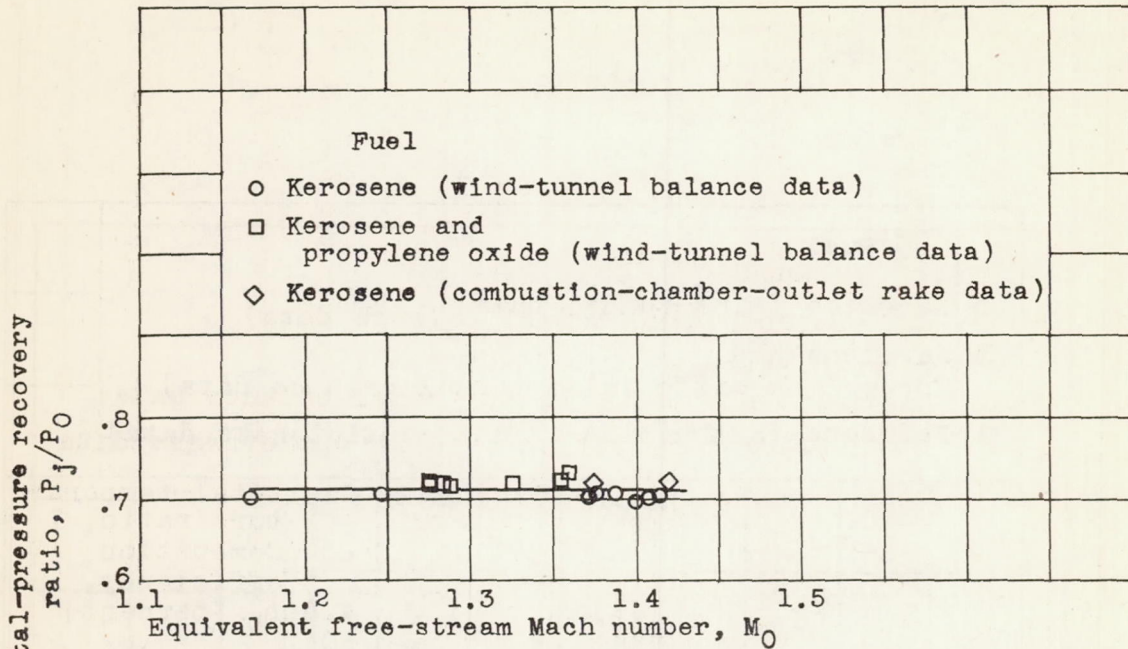


Figure 14. - Effect of equivalent free-stream Mach number on total-pressure recovery ratio across the engine; range of gas total-temperature ratio, 3.6 to 5.4.

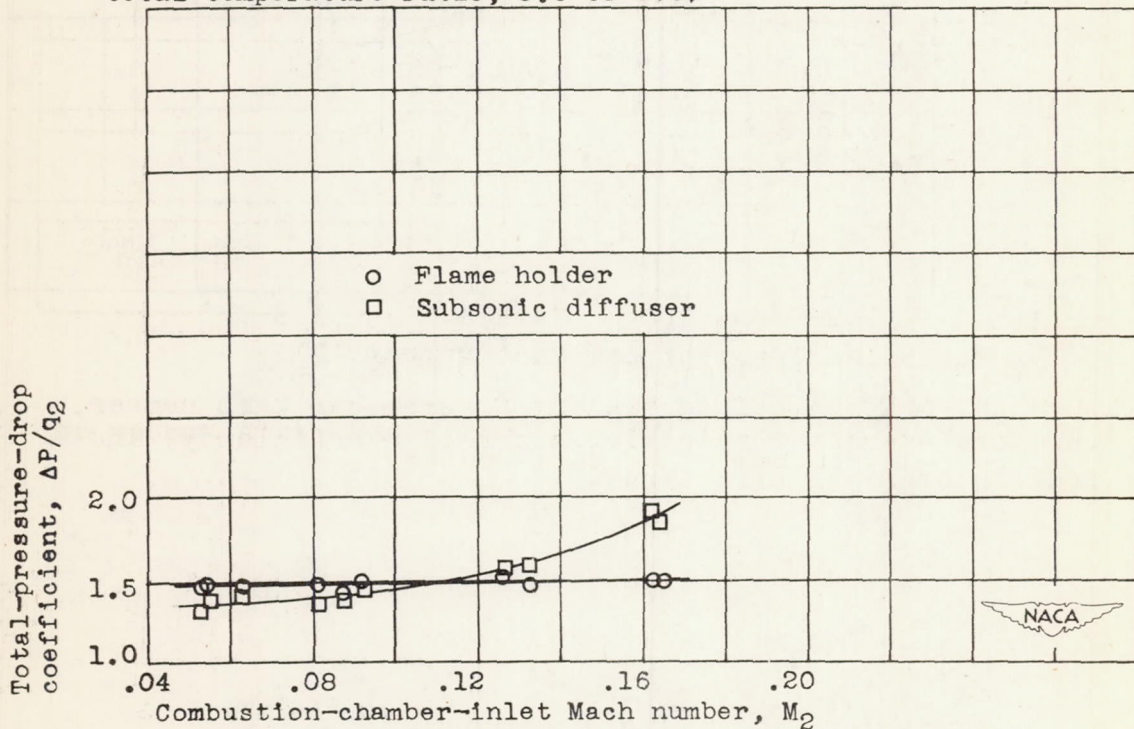


Figure 15. - Effect of combustion-chamber-inlet Mach number on total-pressure-drop coefficient for flame holder and subsonic diffuser.

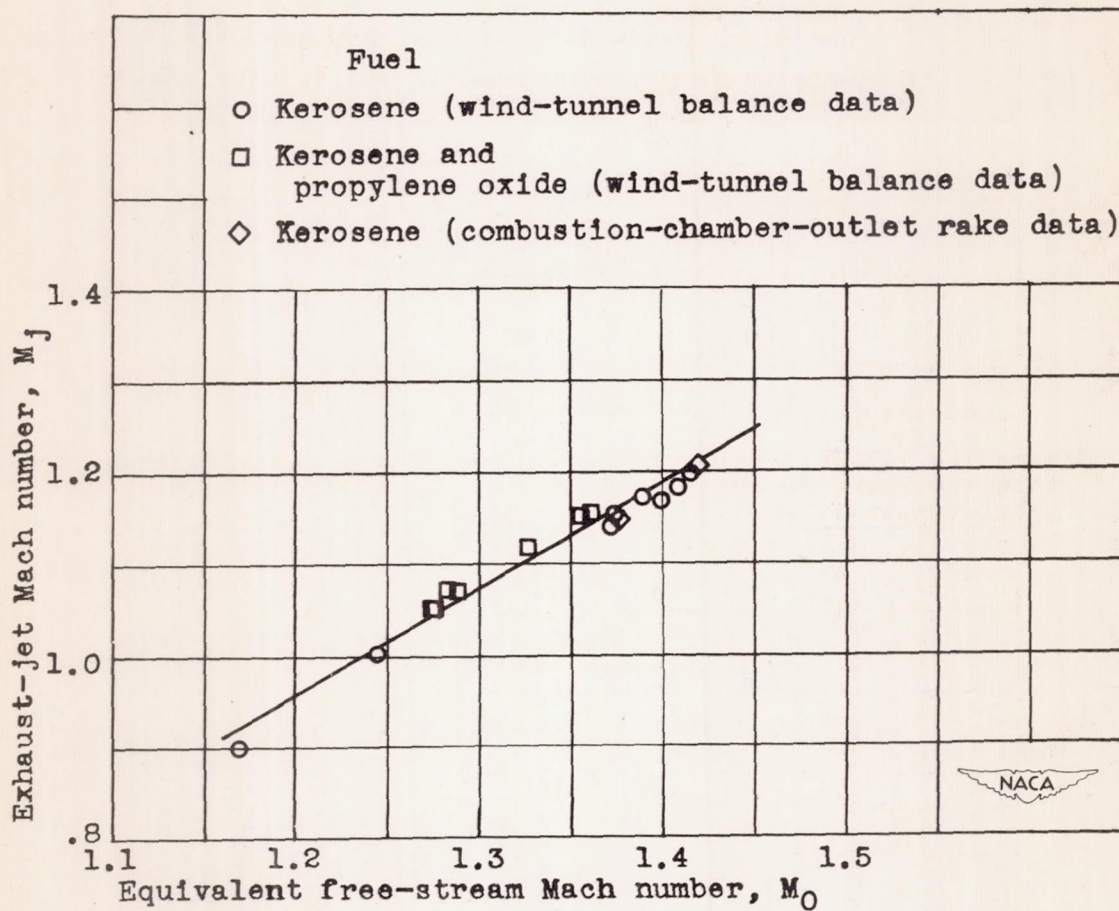


Figure 16. - Effect of equivalent free-stream Mach number on exhaust-jet Mach number.

1910

1911

1912

1913

1914

1915

1916

1917

1918

1919

1920

1921

1922

1923

1924

1925

1926

1927

1928

1929

1930

1931

1932

1933

1934

1935

1936

1937

1938

1939

1940

1941

1942

1943

1944

1945

1946

1947

1948

1949

1950

1951

1952

1953

1954

1955

1956

1957

1958

1959

1960

1961

1962

1963

1964

1965

1966

1967

1968

1969

1970

1971

1972

1973

1974

1975

1976

1977

1978

1979

1980

1981

1982

1983

1984

1985

1986

1987

1988

1989

1990

1991

1992

1993

1994

1995

1996

1997

1998

1999

2000

2001

2002

2003

2004

2005

2006

2007

2008

2009

2010

2011

2012

2013

2014

2015

2016

2017

2018

2019

2020

2021

2022

2023

2024

2025

2026

2027

2028

2029

2030

2031

2032

2033

2034

2035

2036

2037

2038

2039

2040

2041

2042

2043

2044

2045

2046

2047

2048

2049

2050

Year	Jan	Feb	Mar	Apr	May	Jun	Jul	Aug	Sep	Oct	Nov	Dec
1910												
1911												
1912												
1913												
1914												
1915												
1916												
1917												
1918												
1919												
1920												
1921												
1922												
1923												
1924												
1925												
1926												
1927												
1928												
1929												
1930												
1931												
1932												
1933												
1934												
1935												
1936												
1937												
1938												
1939												
1940												
1941												
1942												
1943												
1944												
1945												
1946												
1947												
1948												
1949												
1950												
1951												
1952												
1953												
1954												
1955												
1956												
1957												
1958												
1959												
1960												
1961												
1962												
1963												
1964												
1965												
1966												
1967												
1968												
1969												
1970												
1971												
1972												
1973												
1974												
1975												
1976												
1977												
1978												
1979												
1980												
1981												
1982												
1983												
1984												
1985												
1986												
1987												
1988												
1989												
1990												
1991												
1992												
1993												
1994												
1995												
1996												
1997												
1998												
1999												
2000												
2001												
2002												
2003												
2004												
2005												
2006												
2007												
2008												
2009												
2010												
2011												
2012												
2013												
2014												
2015												
2016												
2017												
2018												
2019												
2020												
2021												
2022												
2023												
2024												
2025												
2026												
2027												
2028												
2029												
2030												
2031												
2032												
2033												
2034												
2035												
2036												
2037												
2038												
2039												
2040												
2041												
2042												
2043												
2044												
2045												
2046												
2047												
2048												
2049												
2050												